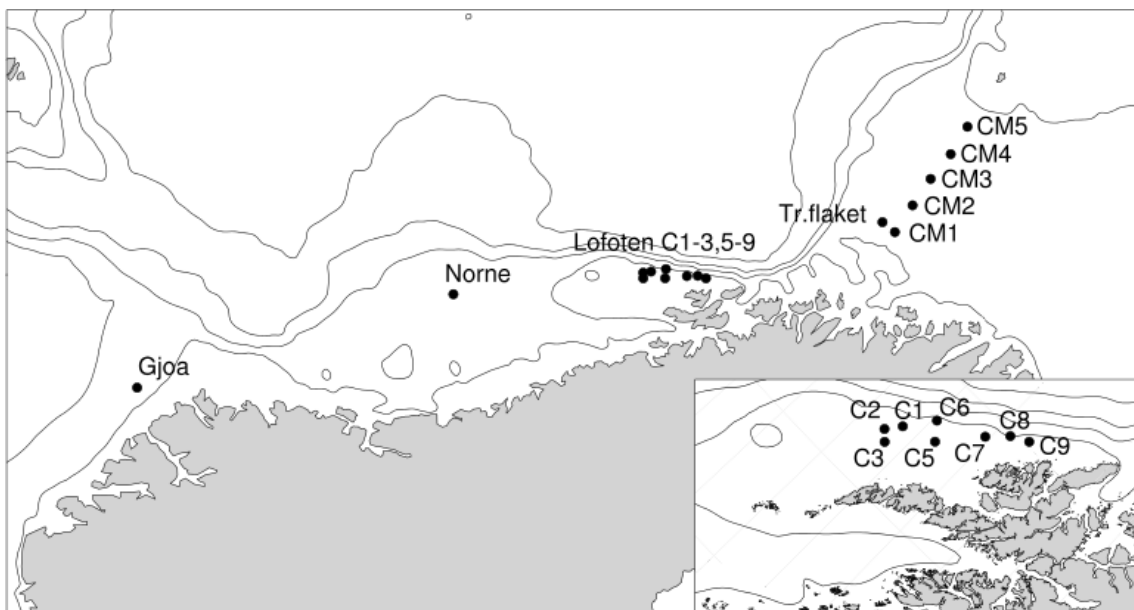




Evaluation of ocean currents from model simulations

Arne Melsom, Yvonne Gusdal





Norwegian
Meteorological
Institute

METreport

Title Evaluation of ocean currents from model simulations	Date April 17, 2015
Section Ocean and ice	Report no. 14/2015
Author(s) Arne Melsom, Yvonne Gusdal	Classification <input checked="" type="radio"/> Free <input type="radio"/> Restricted
Client(s) The Research Council of Norway	Client's reference
Abstract <p>In various projects during recent years, archives with results from ocean circulation models have been established. Here, we evaluate the quality of the ocean current archives, using observations from moored current meters from selected positions along the Norwegian coast. We limit this examination to the statistical representativeness of the model results for observed conditions. For this purpose, we display validation results in the form of quantile-quantile plots, probability distributions of current speed and direction, and distribution of end positions of progressive vectors. In addition, summary results are given in tabulated formats. We investigate results from two hindcast archives, which we refer to as SVIM and NoSH. These hindcasts were both produced by the ROMS ocean model. We find that results from these experiment have their strength and weaknesses in the same regions, with relatively high quality in the region of the Barents Sea opening, and relatively low quality near the shelf break off the Lofoten archipelago. Moreover, the more recent of the two simulations, NoSH, perform slightly better when it comes to reproducing the statistical distribution of the observed currents.</p>	
Keywords ocean currents, validation	

Disciplinary signature
Lars Anders Breivik

Responsible signature
Øystein Hov

Abstract

In various projects during recent years, archives with results from ocean circulation models have been established. Here, we evaluate the quality of the ocean current archives, using observations from moored current meters from selected positions along the Norwegian coast. We limit this examination to the statistical representativeness of the model results for observed conditions. For this purpose, we display validation results in the form of quantile-quantile plots, probability distributions of current speed and direction, and distribution of end positions of progressive vectors. In addition, summary results are given in tabulated formats. We investigate results from two hindcast archives, which we refer to as SVIM and NoSH. These hindcasts were both produced by the ROMS ocean model. We find that results from these experiment have their strength and weaknesses in the same regions, with relatively high quality in the region of the Barents Sea opening, and relatively low quality near the shelf break off the Lofoten archipelago. Moreover, the more recent of the two simulations, NoSH, perform slightly better when it comes to reproducing the statistical distribution of the observed currents.

Contents

1	Introduction	5
2	Methods	5
3	Atlas of ocean current statistics	8
3.1	IMR stations	8
3.1.1	CM1	10
3.1.2	CM2	11
3.1.3	CM3	12
3.1.4	CM4	13
3.1.5	CM5	14
3.2	Offshore industry stations	15
3.2.1	Gjøa	17
3.2.2	Norne	18
3.2.3	Lofoten C1	19
3.2.4	Lofoten C2	20
3.2.5	Lofoten C3	21
3.2.6	Lofoten C5	22
3.2.7	Lofoten C6	23
3.2.8	Lofoten C7	24
3.2.9	Lofoten C8	25
3.2.10	Lofoten C9	26
3.2.11	Tromsoflaket	27
4	Discussion	28

1 Introduction

In recent years, several ocean circulation hindcast archives have been produced at MET Norway, in collaboration with the Institute of Marine Research (IMR). The archives have been initialized from climatology, and subsequently forced with results from atmospheric reanalyses. The main purpose of establishing such archives is to provide representations of the oceanographic conditions on which other applications are based, such as primary production models and met-ocean conditions for offshore activities.

This report evaluates the results for ocean currents from two of these archives, hereafter referred to as the SVIM¹ archive, and the NoSH² archive. Both of these archives were produced on a 4 km grid on a polar stereographic projection. Additional evaluation of the SVIM archive is provided by Lien et al. (2013), and similarly, a detailed evaluation of the NoSH archive is given by Røed et al. (2015).

2 Methods

In the present report, we compare model results for ocean currents with observations from moored current meters at positions off the coast of central and northern Norway. The positions of these observations are displayed along with a depiction of the model domain in Figure 1. The observations represent currents at various depths that in general differ between the mooring sites. However, observations for the 50 m level are available from nearly all sites. Hence, the present investigation is performed using the data and corresponding model results from this level.

We acknowledge that in the absence of data with a mesoscale resolution, it is not possible to accurately describe the observed history. Our aim becomes to compare the statistics of the observed and modeled currents. In doing so, we investigate daily averaged currents. In Section 3, probability distribution functions (p.d.f.s) for the current speed and direction are displayed, along with quantile-quantile (qq) plots, all for the daily averaged currents. We also include tabulated values for

- slopes of the regression lines (=1 for a perfect simulation)

¹SVIM: Spatiotemporal Variability In Mortality and growth of fish larvae and zooplankton in the Lofoten-Barents Sea ecosystem

²NoSH: Norwegian Sea Hindcast

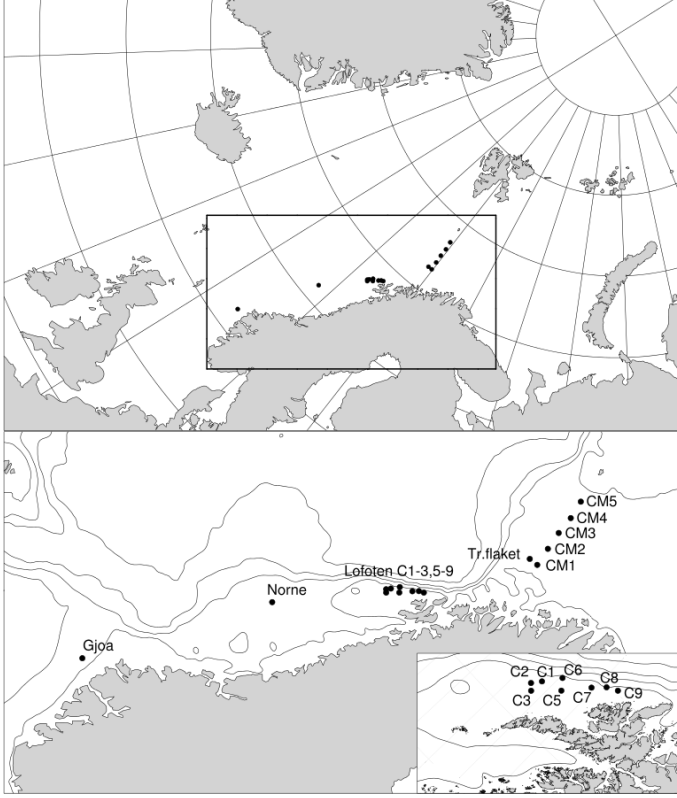


Figure 1: Top: Domain of the NoSH archive. The SVIM domain is nearly identical. The rectangle framed by the black lines is the region displayed below. Black dots correspond to the locations of the current meters. Bottom: Labeled positions from which current meter data were collected and subsequently made available to this study. Inset is a zoomed map for the region of the Lofoten archipelago. Contours correspond to depths of 200 m, 500 m, 1000 m and 2000 m.

- mean deviation of the qq curve from the regression line ($\bar{\delta}$), nondimensionalised by dividing this deviation by the mean speed from observations ($\overline{v_{obs}}$)

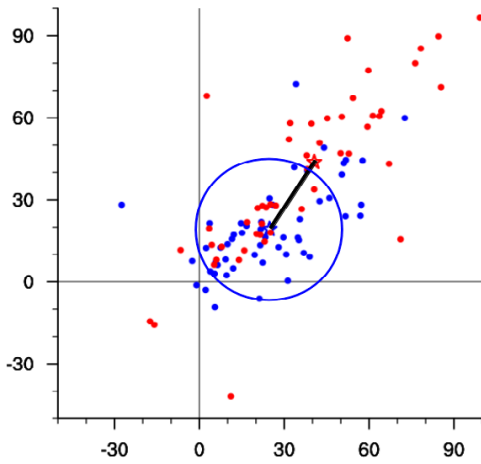
Here, the deviation d of a point (x_0, y_0) from the line $y = a \cdot x + b$ is the shortest distance from the line, which is

$$d^2 = (x_p - x_0)^2 + (y_p - y_0)^2 = (x_p - x_0)^2 + (a \cdot x_p + b - y_0)^2$$

$$d^2_{x_p} = 0 \quad \Rightarrow \quad x_p = \frac{x_0 + a \cdot y_0 - a \cdot b}{1 + a^2}$$

It is of considerable interest also to examine drift statistics over consecutive days, weeks and even months, with applications like drift of larvae, oil spills and icebergs in mind. However, the lengths of the time series are generally too short for an investigation of the drift statistics over long periods, as the sample sizes become small.

Moreover, since the observations are from fixed sites, they represent the Eulerian mean rather than (Lagrangian) drift. Nevertheless, to gain some information on time scales somewhat longer than a day, we compare the end position of progressive vectors for a period of 5 days. The distributions at the various mooring positions are shown in figures in Section 3, where we also include tables with over-all statistics of the 5-day progressive



• Figure 2: Illustration figure for statistical properties. Displayed here are end points of 5-day progressive vectors from observations (blue dots) and model results (red dots), from the Lofoten C5 location. The asterisks denote the respective mean positions (centers of gravity) of the two sets of end points. The blue circle shows the extent of one standard deviation offset for the observations. The black line is simply the vector offset between the mean positions from model results and observations.

vector end points.

These statistics include results for

- the average (center of gravity) progressive vector end positions from observations, NoSH archive results and SVIM archive results (asterisks in the illustration in Figure 2)
- the distance between the observed center of gravity and those derived from the archives (Δ_N, Δ_S , respectively; black line in Figure 2)
- the standard deviation of the distance from the progressive vector end points to the centers of gravity for observations (σ_{obs}), NoSH results (σ_N) and SVIM results (σ_S) (radius of the blue circle in Figure 2)
- non-dimensional center of gravity distances, computed as the ratio of the distance to the standard deviation distance of the observations (*i.e.*, Δ_N/σ_{obs} , Δ_S/σ_{obs} ; slightly more than 1 in Figure 2)

3 Atlas of ocean current statistics

In this section, we present tables and figures based on which we will be able to evaluate the results for each observational position. The results given here will be discussed in Section 4. Results are limited to time periods from which both observations and model results are available.

The p.d.f.s display no. of occurrences of daily mean velocities, with the full span divided into 20 bins of equal size. Bins are displaced by one half bin, so that e.g. the no. of occurrence given on the vertical axis for a speed of 0 cm/s corresponds to no. of occurrences in the interval $0 - 1/40^{th}$. The color coding of the various curves are given by the in-set labels. Due to questionable data quality for low current speeds, observations and model results with speeds less than 2 cm/s were discarded prior to this analysis.

In the quantil-quantile (qq) plots, both observations and model results of the daily mean currents were sorted by magnitude. The match-ups are plotted as +s in the qq plots. These curves can then be used to assess the model’s capability to reproduce the observed statistical distribution. A regression line is then determined as a least square linear fit to the qq curve. We also include dots for match-ups in time, in order to subsequently assess the model’s capability of reproducing the observed history.

3.1 IMR stations

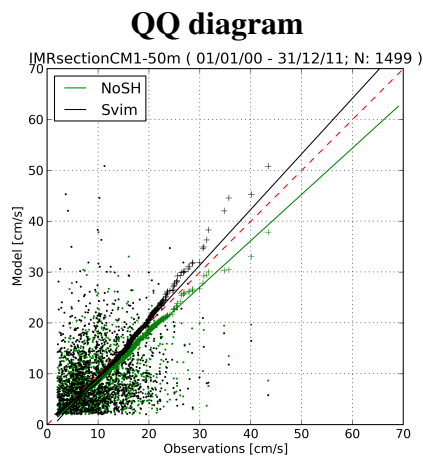
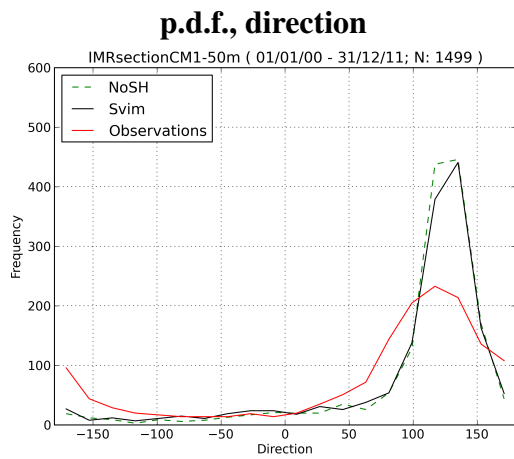
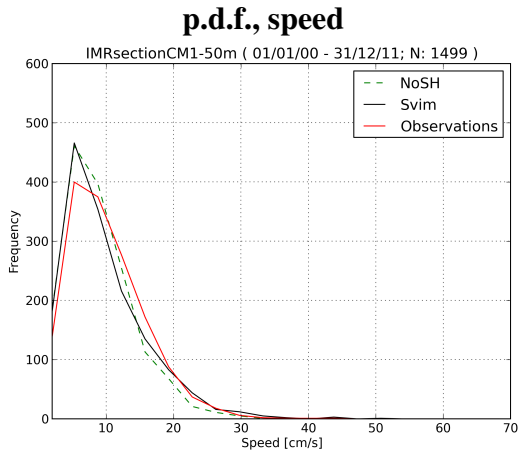
Position	Period	NoSH		SVIM	
		slope	deviation	slope	deviation
CM1	2003-02-21 - 2011-04-12	0.91	0.015	1.10	0.031
CM2	2000-01-01 - 2011-12-31	1.12	0.019	1.22	0.026
CM3	2000-01-01 - 2011-12-31	0.92	0.017	0.77	0.018
CM4	2003-03-01 - 2011-12-31	1.16	0.021	0.83	0.025
CM5	2003-10-01 - 2011-12-31	0.96	0.015	0.70	0.026

Table 1: Slope of regression line for qq curves, and nondimensional mean deviation from regression line ($\bar{\delta}/\overline{v_{obs}}$). Dates listed under Period are first and last dates with data, but the time series may have gaps. See Section 2 for more information.

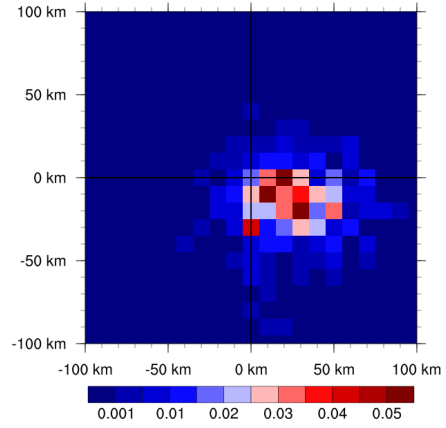
Position	#end points	\bar{x}_{obs} \bar{y}_{obs}	\bar{x}_N \bar{y}_N	\bar{x}_S \bar{y}_S	Δ_N	Δ_S	σ_{obs}	σ_N	σ_S	Δ_N/σ_{obs}	Δ_S/σ_{obs}
CM1	357	23.1 -15.2	27.3 -18.3	25.1 -18.0	5.2	3.5	27.9	28.7	27.6	0.19	0.13
CM2	650	14.9 -9.8	32.2 -17.4	22.3 -14.2	19.0	8.6	27.7	36.4	32.4	0.69	0.31
CM3	643	15.2 -6.5	2.0 -15.1	5.5 -10.9	15.8	10.7	38.9	49.4	35.3	0.41	0.27
CM4	521	12.8 -7.8	24.3 -15.9	12.2 -4.9	14.0	3.0	51.0	61.4	42.5	0.27	0.06
CM5	506	0.6 -8.9	1.1 -7.8	-5.4 -7.9	1.2	6.1	48.1	56.8	35.3	0.02	0.13

Table 2: Statistics of distribution of 5-day progressive vector end points [km]. The quantities are described in detail in Section 2 and Figure 2 therein.

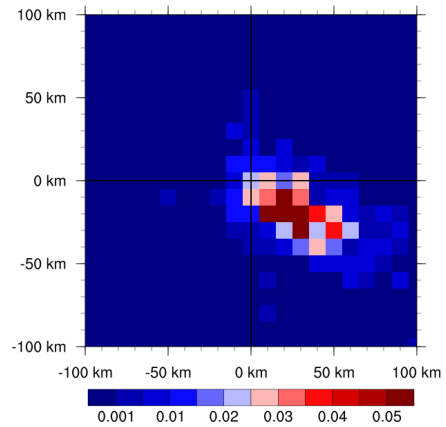
3.1.1 CM1



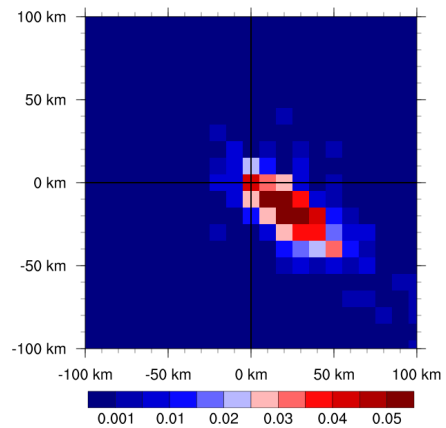
**progressive vectors
observations**



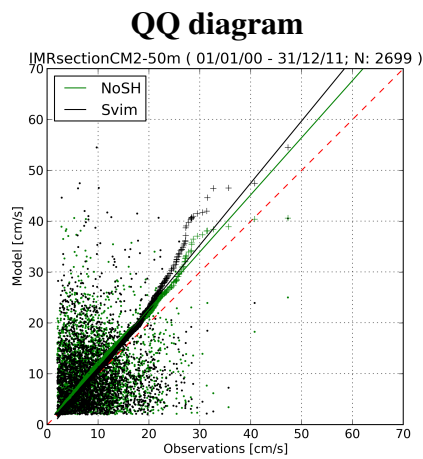
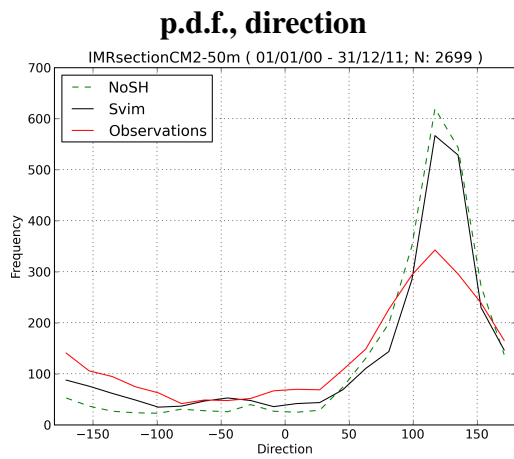
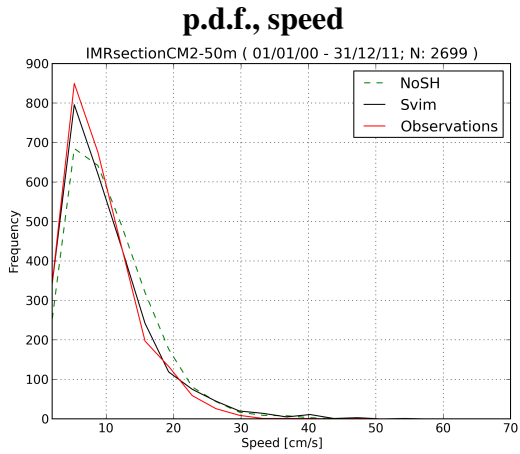
NoSH currents



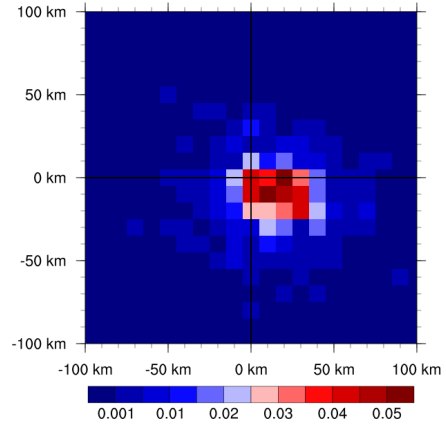
SVIM currents



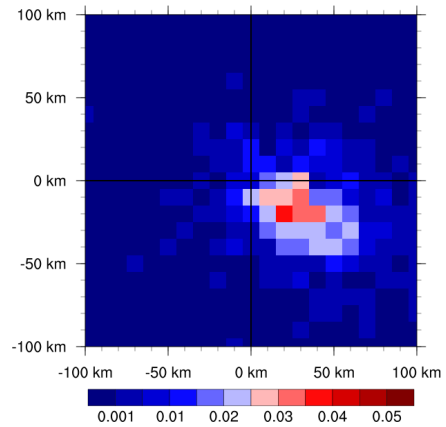
3.1.2 CM2



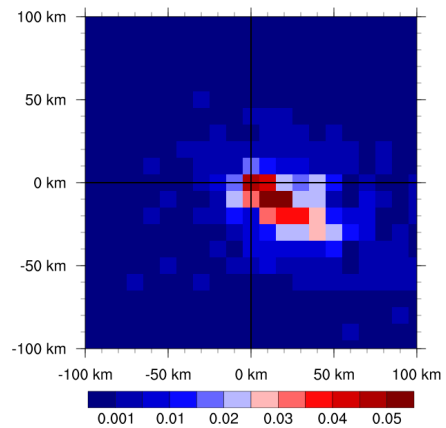
**progressive vectors
observations**



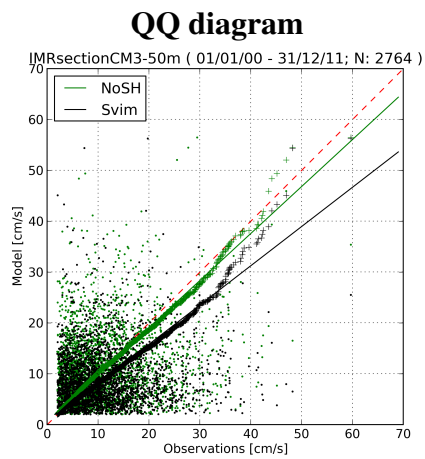
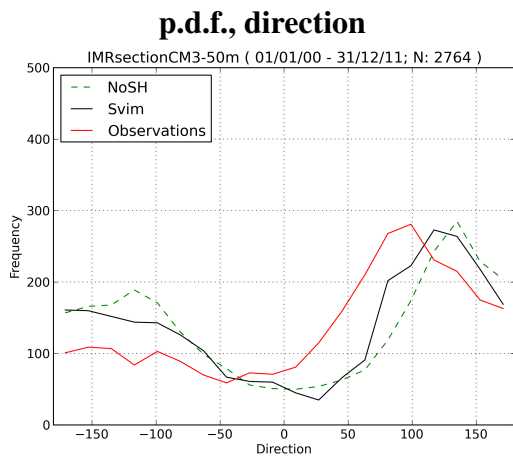
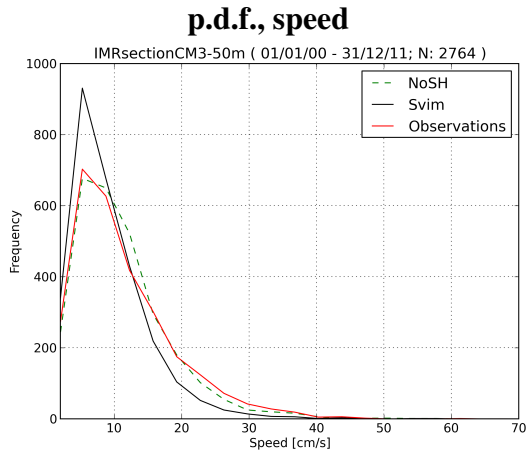
NoSH currents



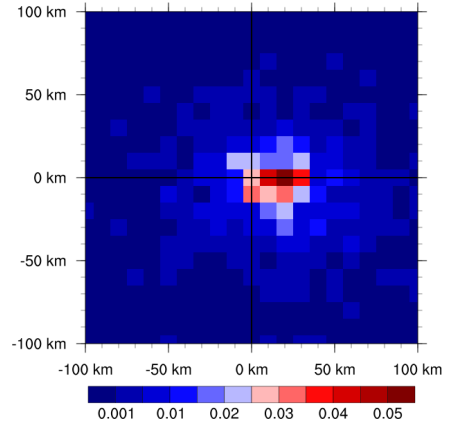
SVIM currents



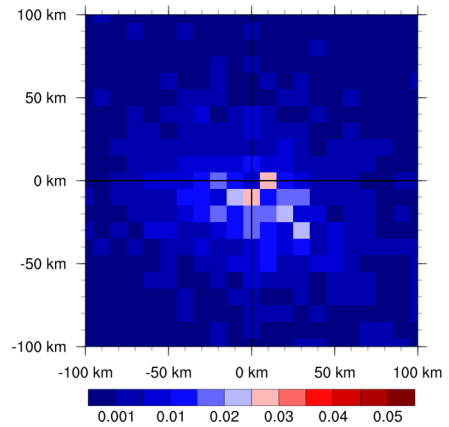
3.1.3 CM3



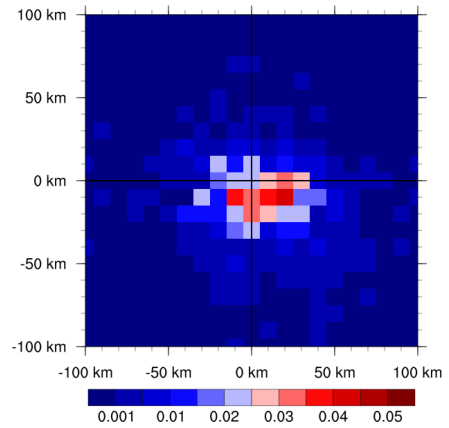
**progressive vectors
observations**



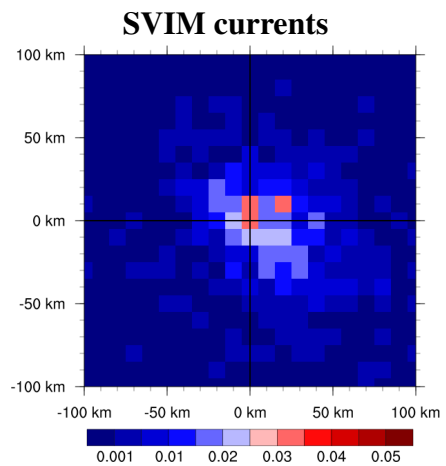
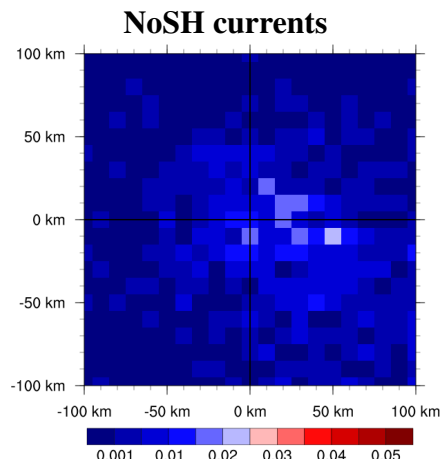
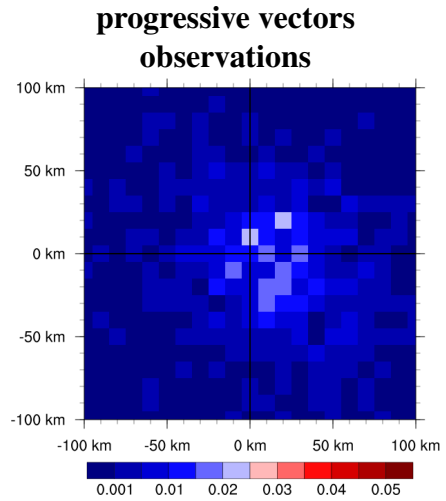
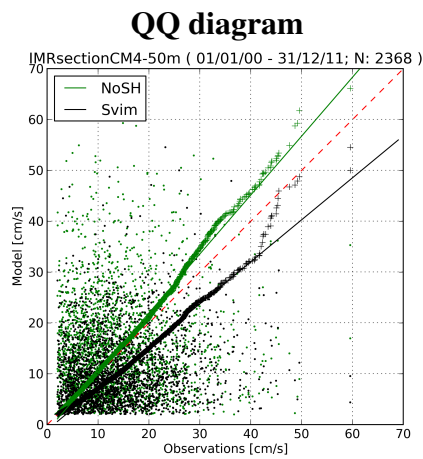
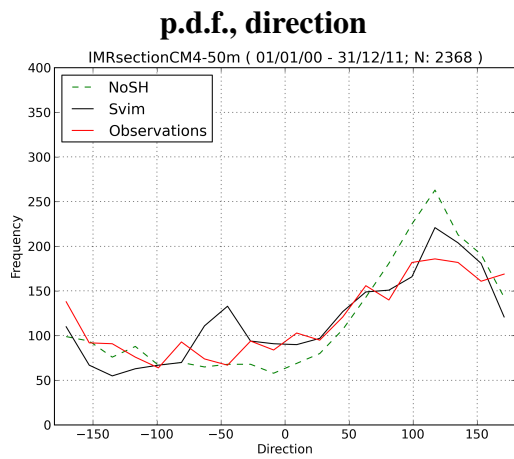
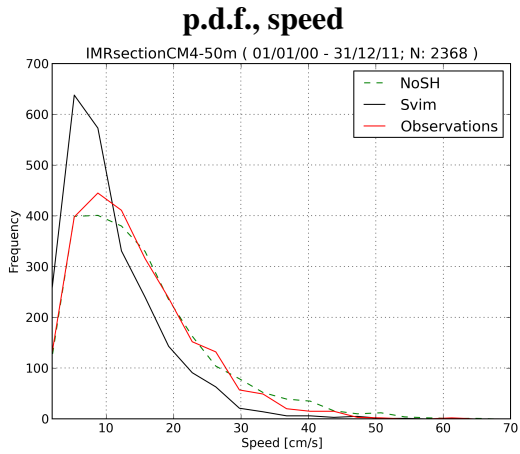
NoSH currents



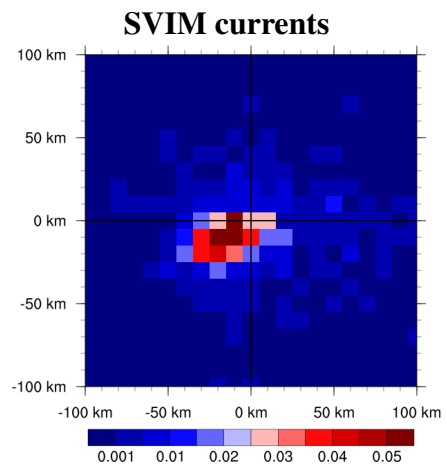
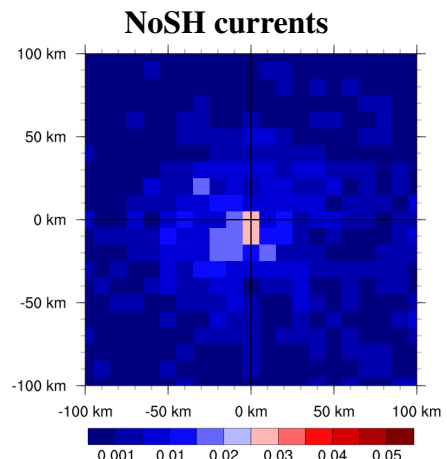
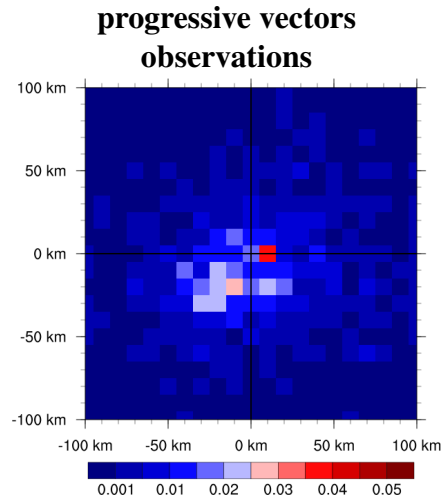
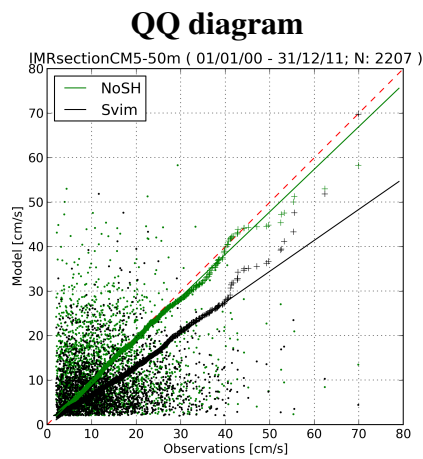
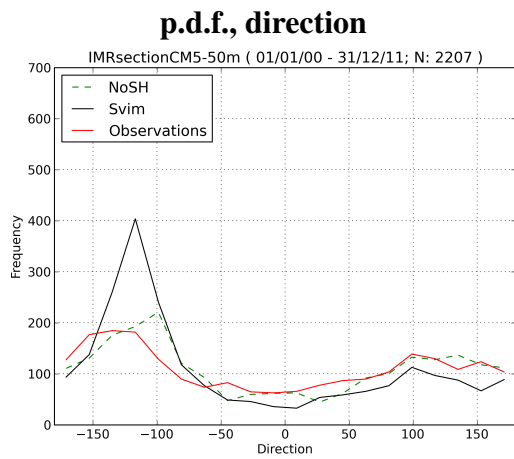
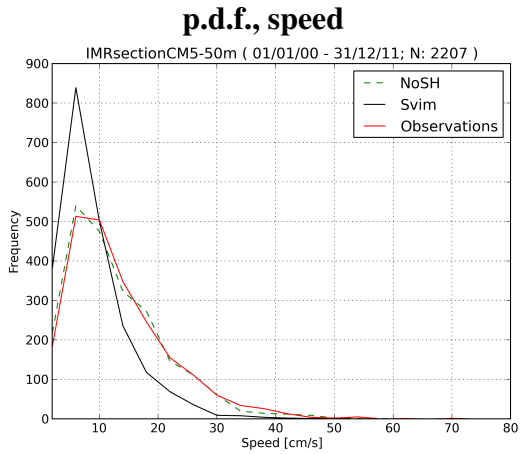
SVIM currents



3.1.4 CM4



3.1.5 CM5



3.2 Offshore industry stations

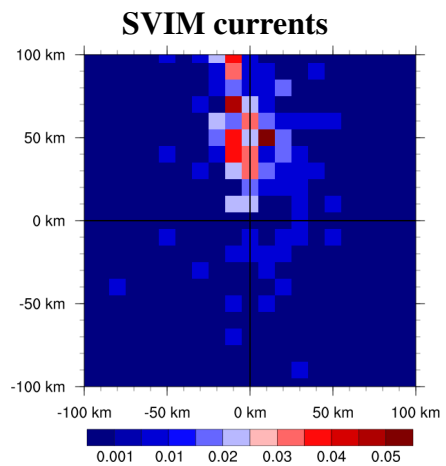
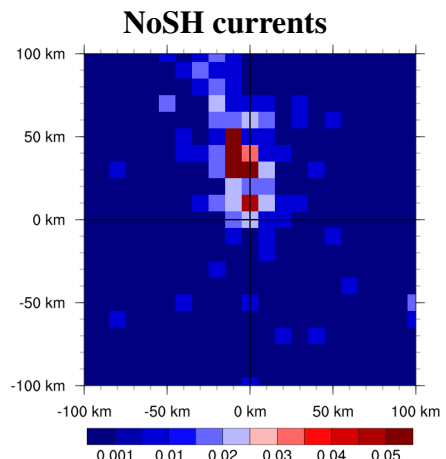
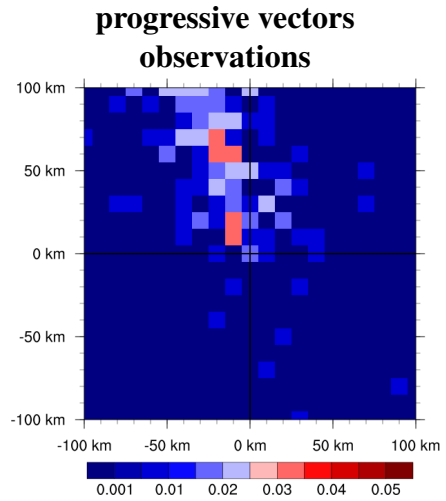
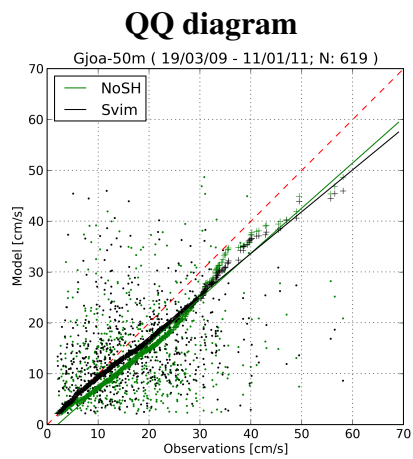
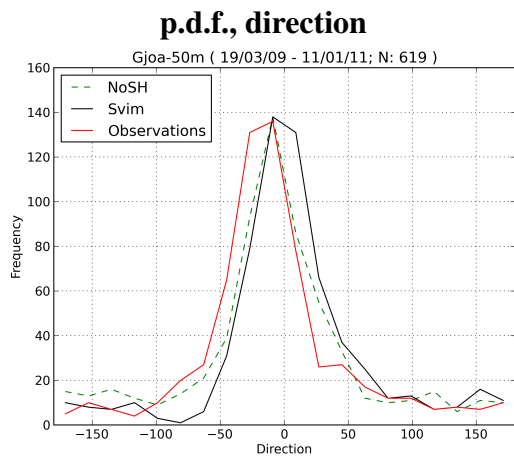
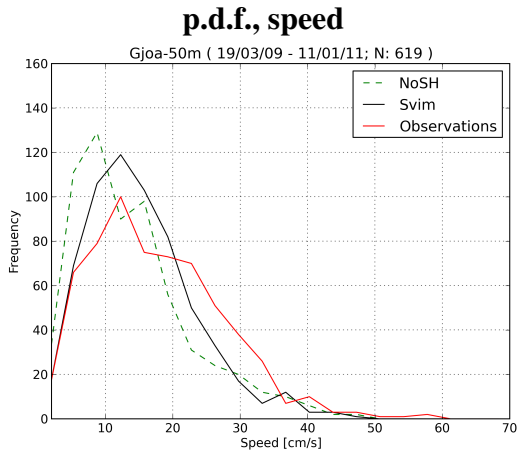
Position	Period	NoSH		SVIM	
		slope	deviation	slope	deviation
Gjøa	2009-03-19 - 2009-04-19	0.89	0.039	0.82	0.020
Norne	1993-09-18 - 1994-06-08	0.58	0.023	0.76	0.034
Lofoten C1	2009-07-13 - 2010-07-30	1.14	0.023	1.28	0.041
Lofoten C2	2009-07-13 - 2010-07-29	1.67	0.030	2.00	0.028
Lofoten C3	2009-07-13 - 2010-07-30	1.50	0.043	1.45	0.031
Lofoten C5	2009-07-13 - 2010-07-03	1.75	0.029	1.74	0.031
Lofoten C6	2009-07-13 - 2010-07-29	1.75	0.054	2.17	0.066
Lofoten C7	2009-07-13 - 2010-07-29	1.25	0.040	1.40	0.056
Lofoten C8	2009-07-13 - 2010-07-29	2.14	0.052	2.20	0.129
Lofoten C9	2009-07-13 - 2010-07-29	1.22	0.020	1.37	0.024
Tromsøflaket	1983-01-02 - 1985-04-02	0.60	0.027	0.61	0.023

Table 3: Slope of regression line for qq curves, and nondimensional mean deviation from regression line ($\bar{\delta}/\sqrt{v_{obs}}$). Dates listed under Period are first and last dates with data, but the time series may have gaps. See Section 2 for more information.

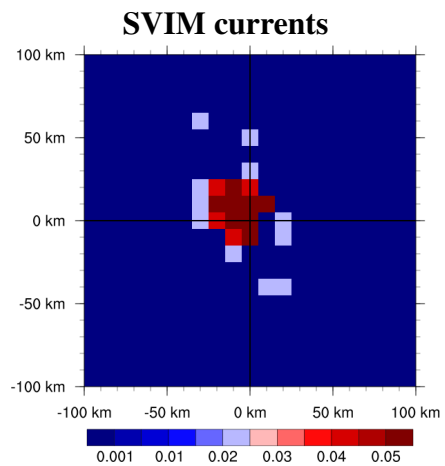
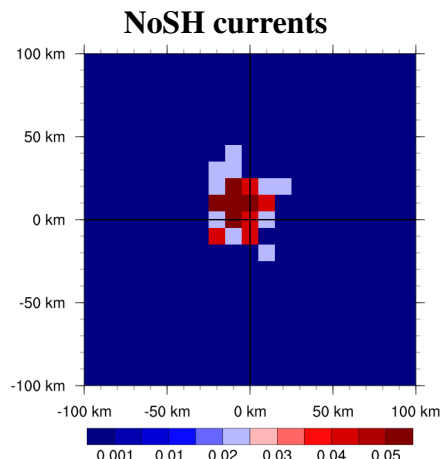
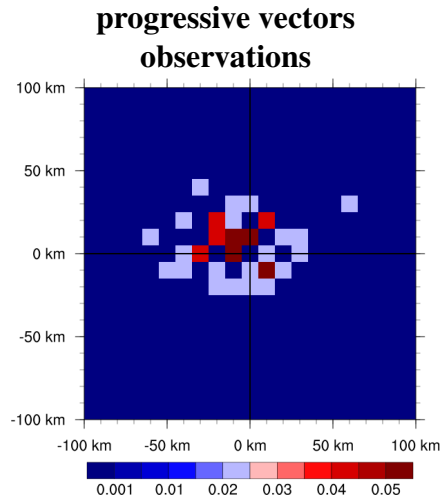
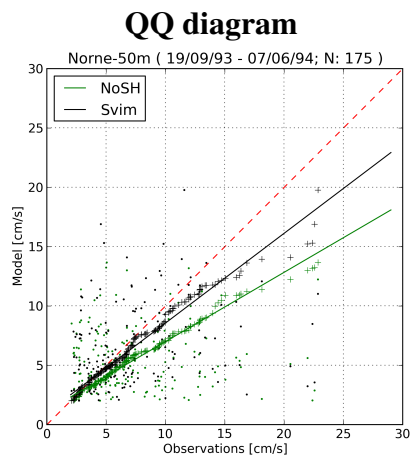
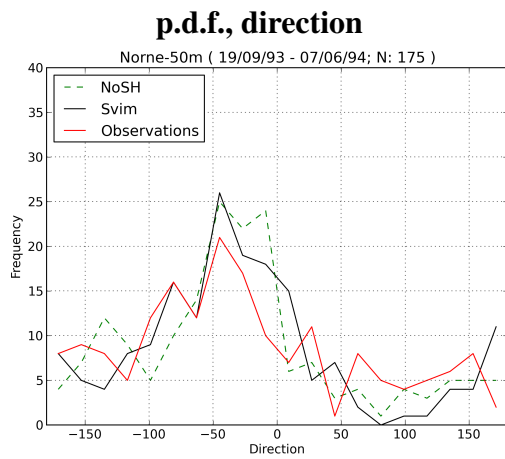
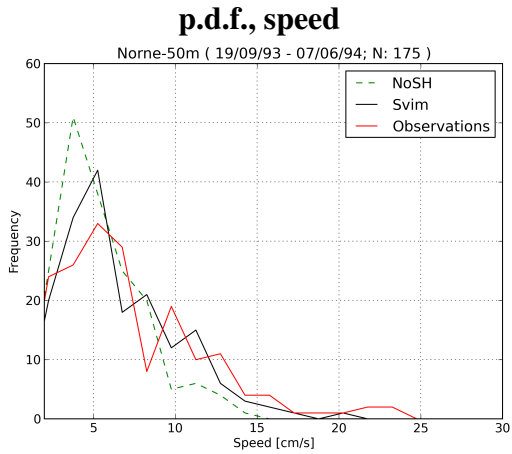
Position	#end points	\bar{x}_{obs} \bar{y}_{obs}	\bar{x}_N \bar{y}_N	\bar{x}_S \bar{y}_S	Δ_N	Δ_S	σ_{obs}	σ_N	σ_S	Δ_N/σ_{obs}	Δ_S/σ_{obs}
Gjøa	130	-14.7 49.9	-3.4 32.2	0.1 44.0	21.1	16.0	49.6	49.1	44.9	0.42	0.32
Norne	49	-8.0 4.0	-6.6 7.7	-6.5 6.0	3.9	2.5	24.3	14.7	20.8	0.16	0.10
Lofoten C1	56	30.7 48.0	62.0 39.2	67.6 30.0	32.5	41.1	34.4	38.7	45.9	0.94	1.19
Lofoten C2	64	17.0 25.8	37.0 34.4	68.3 30.8	21.8	51.6	20.1	39.1	46.5	1.09	2.57
Lofoten C3	76	13.9 11.4	20.0 28.1	17.6 27.5	17.8	16.5	25.8	37.3	37.3	0.69	0.64
Lofoten C5	53	24.8 19.6	40.6 44.0	39.5 39.5	29.1	27.0	25.4	47.7	47.9	1.15	1.07
Lofoten C6	76	49.4 14.3	95.5 77.8	119.5 88.5	78.6	102.1	31.6	50.0	65.4	2.49	3.23
Lofoten C7	64	53.7 7.8	78.3 46.4	105.4 51.7	45.7	67.8	34.9	46.3	50.8	1.31	1.94
Lofoten C8	63	0.7 29.7	80.8 60.7	94.5 75.6	86.3	104.5	20.8	49.1	60.5	4.14	5.02
Lofoten C9	68	84.6 78.1	92.7 89.2	106.5 110.8	16.9	39.4	54.5	67.2	78.2	0.25	0.72
Tromsøflaket	115	17.8 -0.3	20.1 2.5	18.3 4.9	3.7	5.2	34.8	21.3	22.4	0.11	0.15

Table 4: Statistics of distribution of 5-day progressive vector end points [km]. The quantities are described in detail in Section 2 and Figure 2 therein.

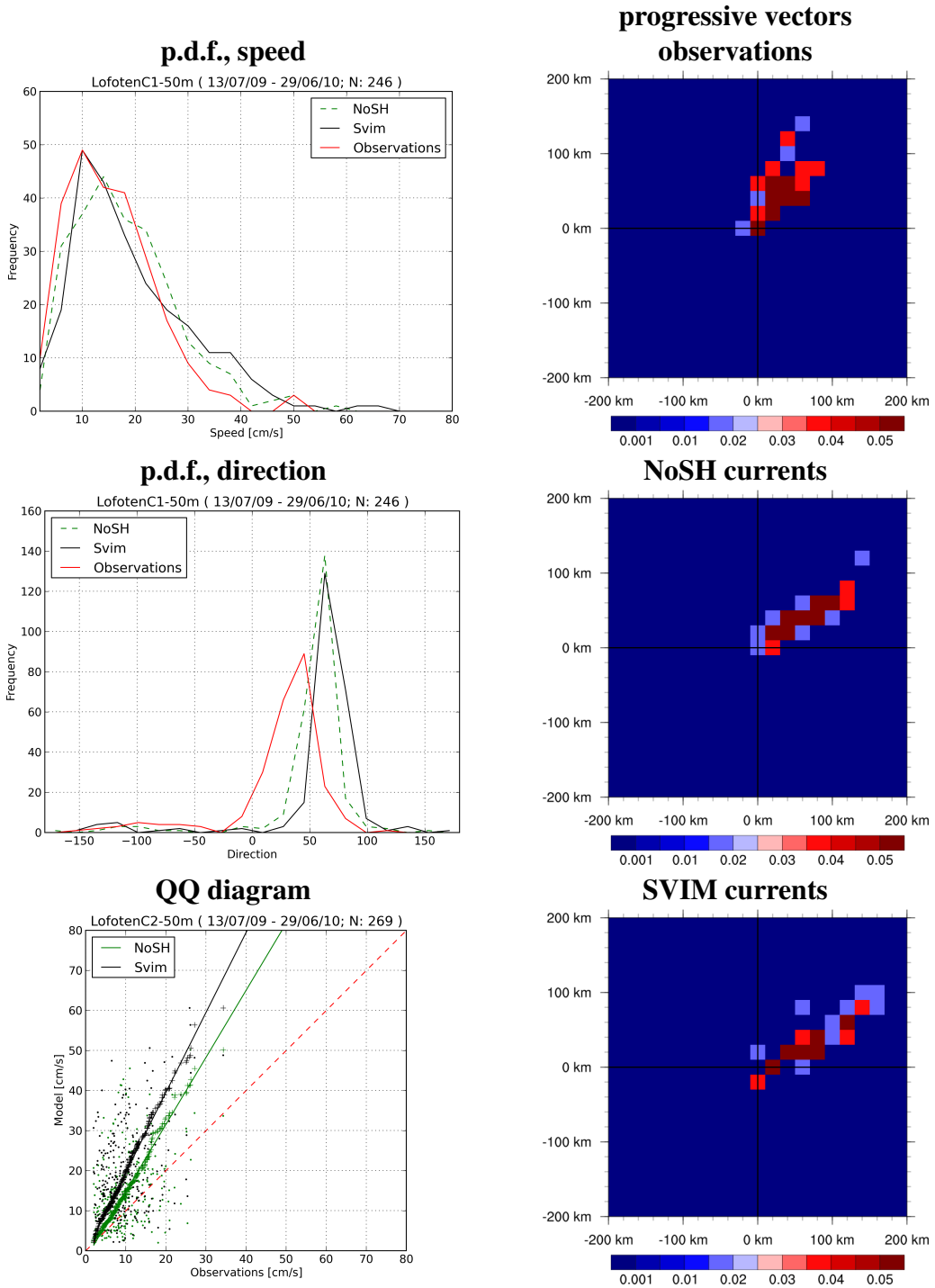
3.2.1 Gjøa



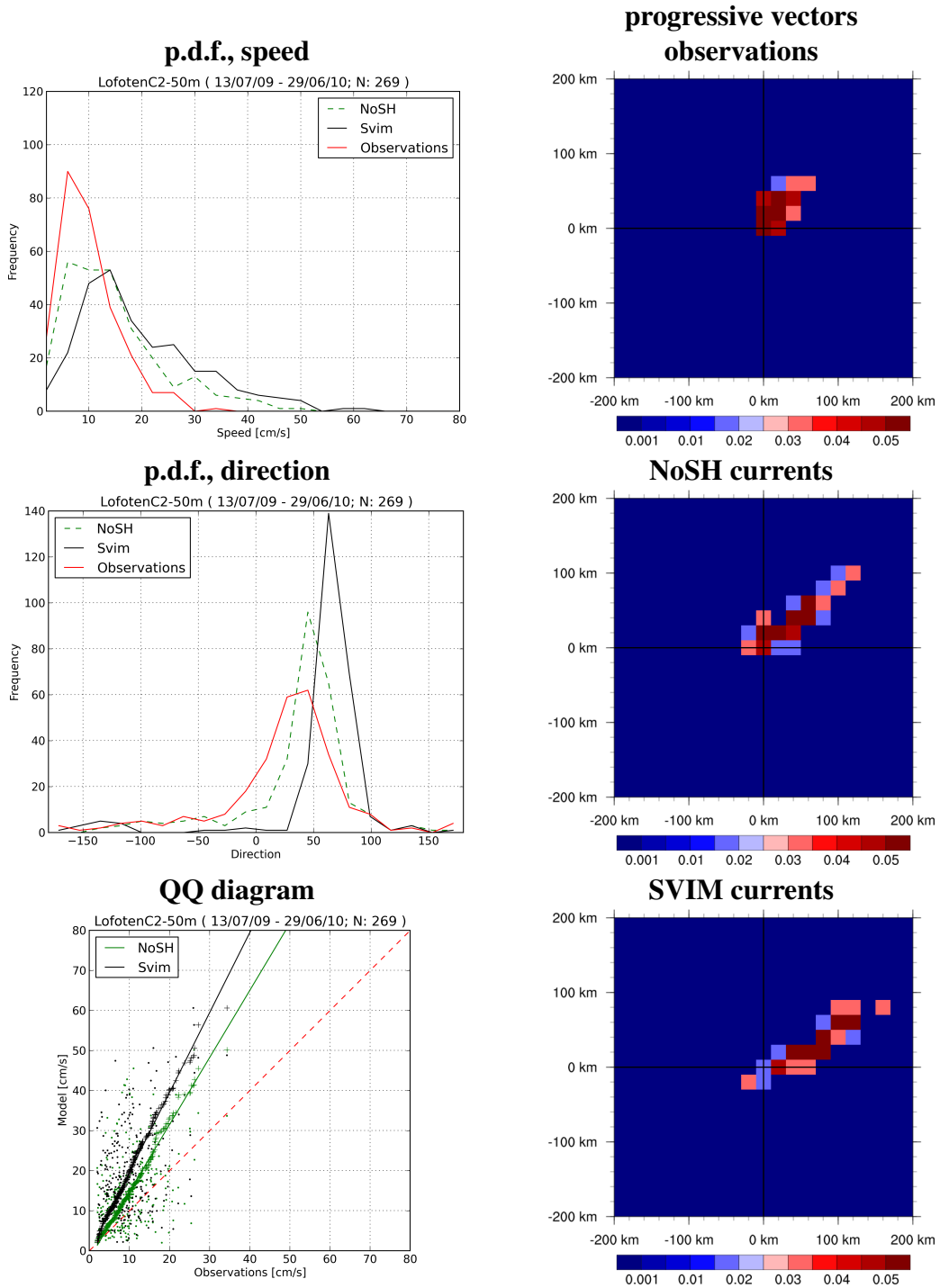
3.2.2 Norne



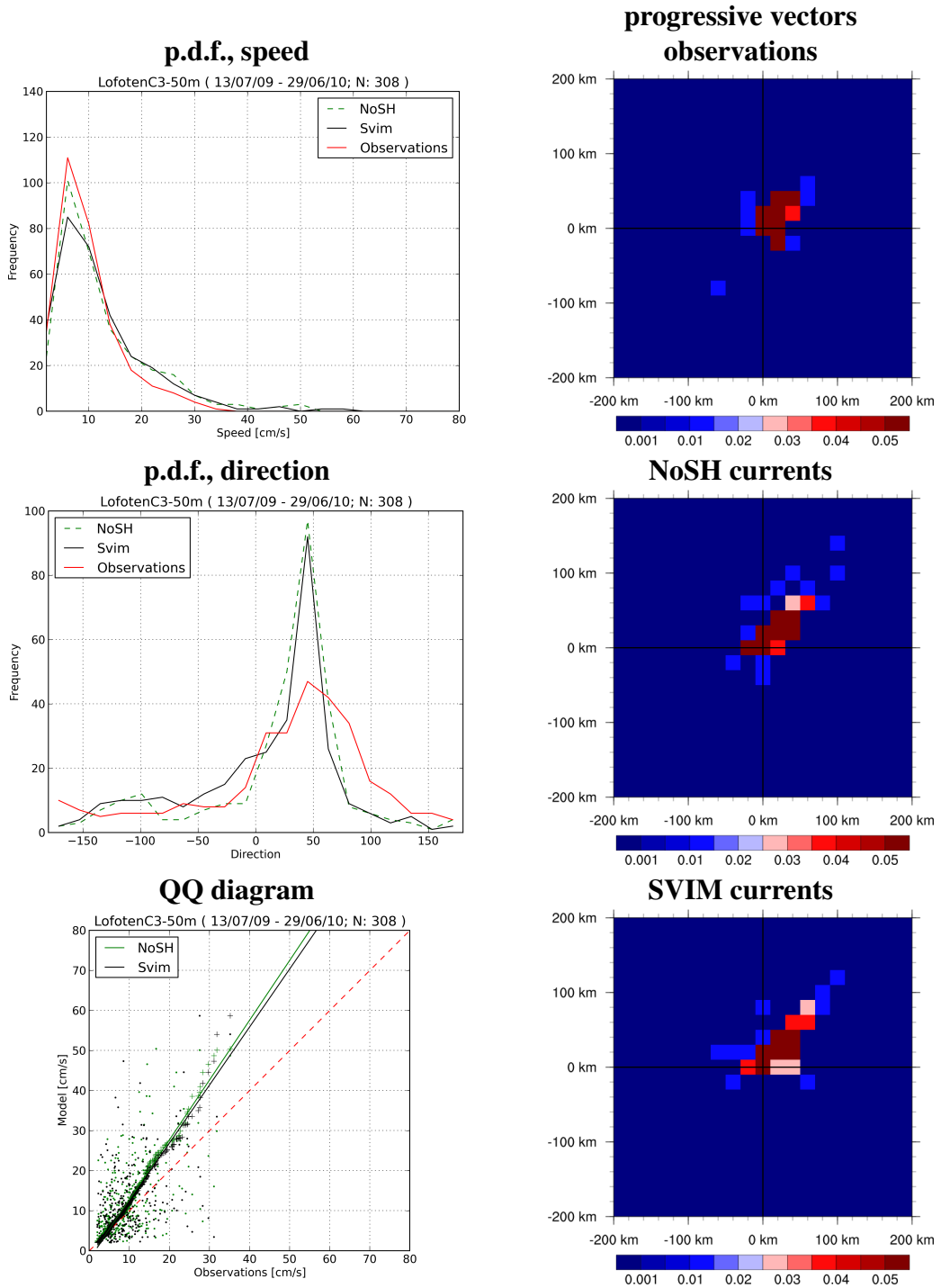
3.2.3 Lofoten C1



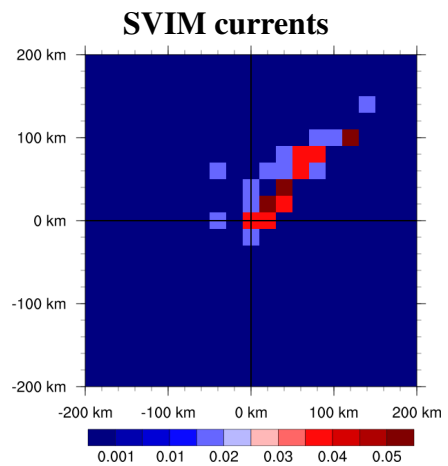
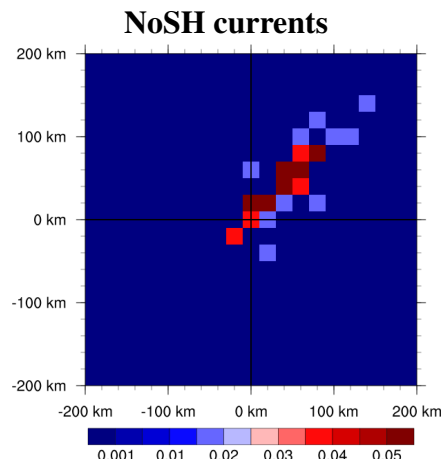
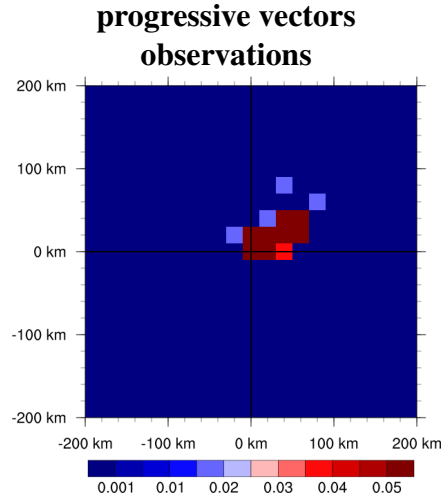
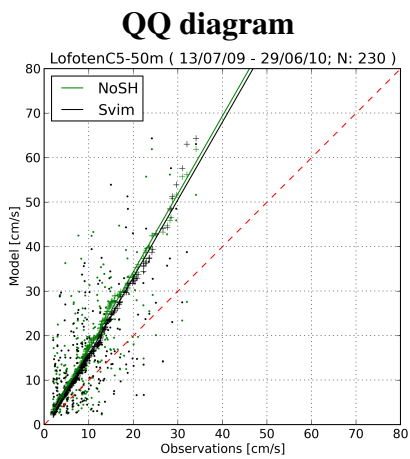
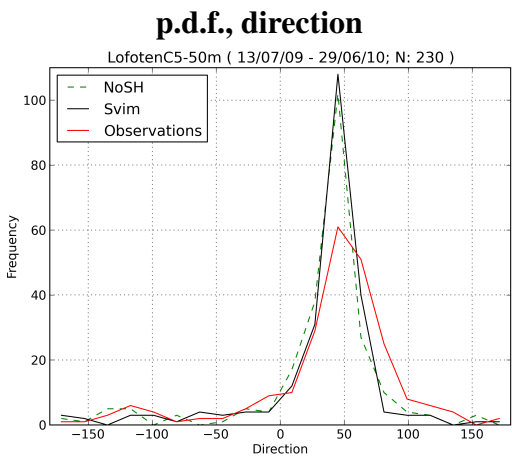
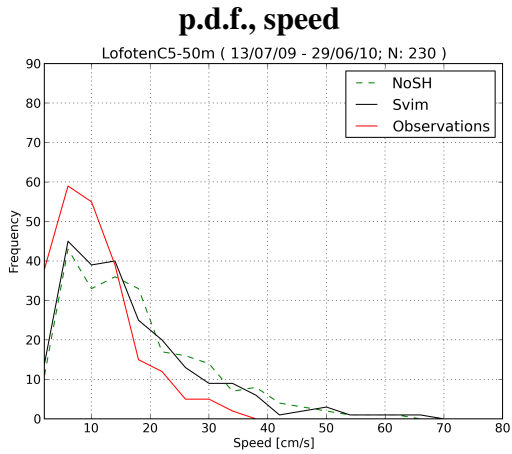
3.2.4 Lofoten C2



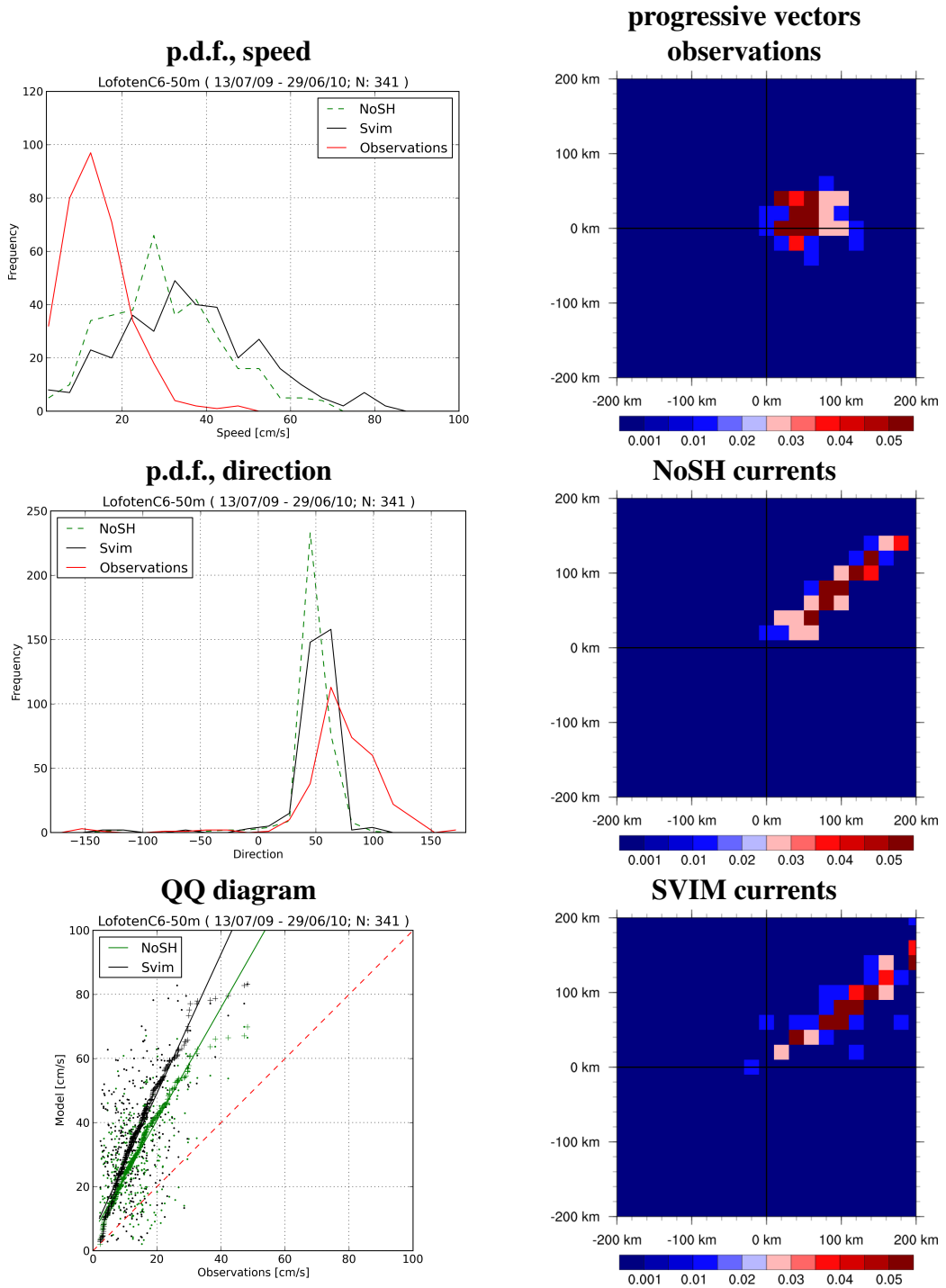
3.2.5 Lofoten C3



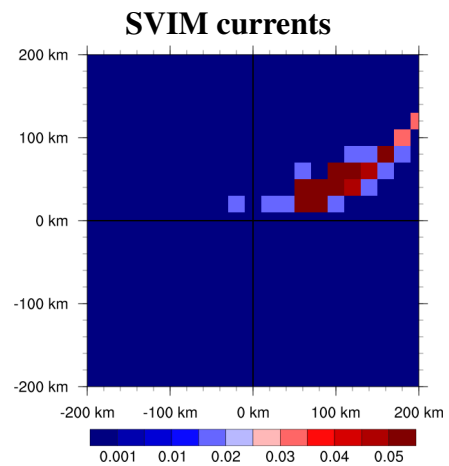
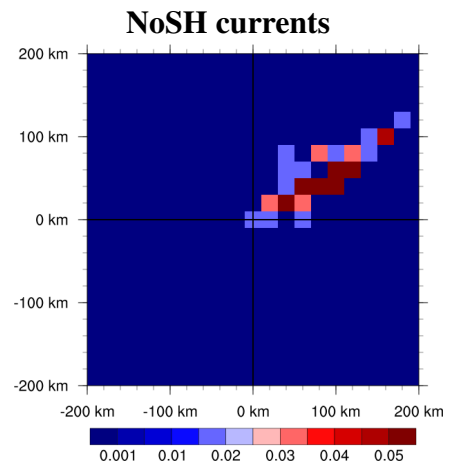
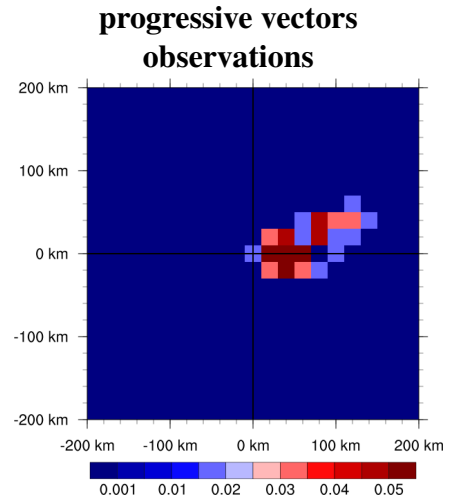
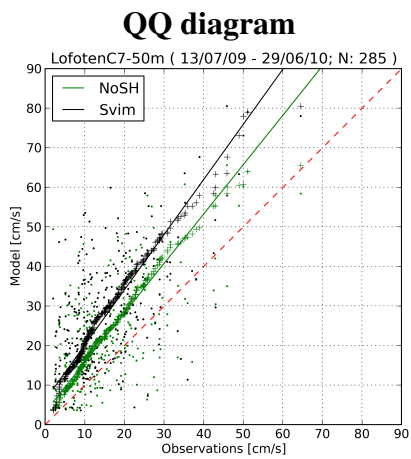
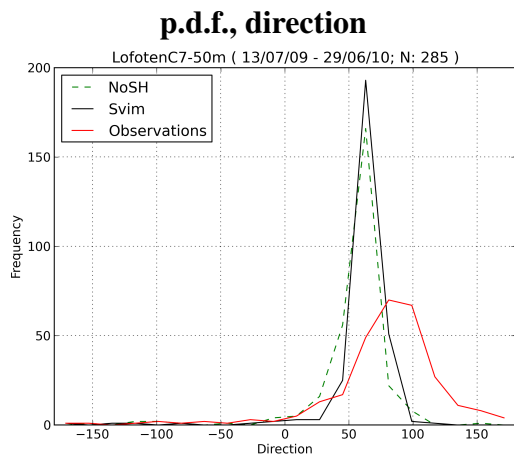
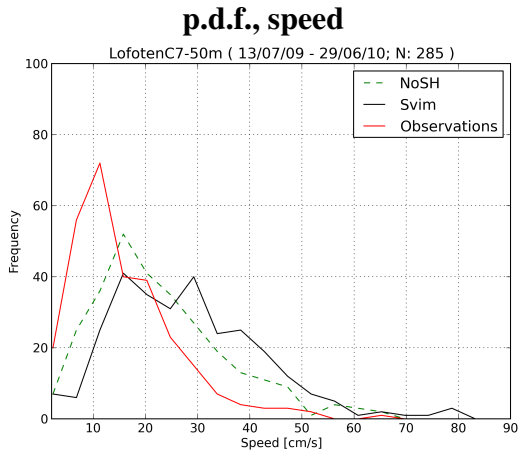
3.2.6 Lofoten C5



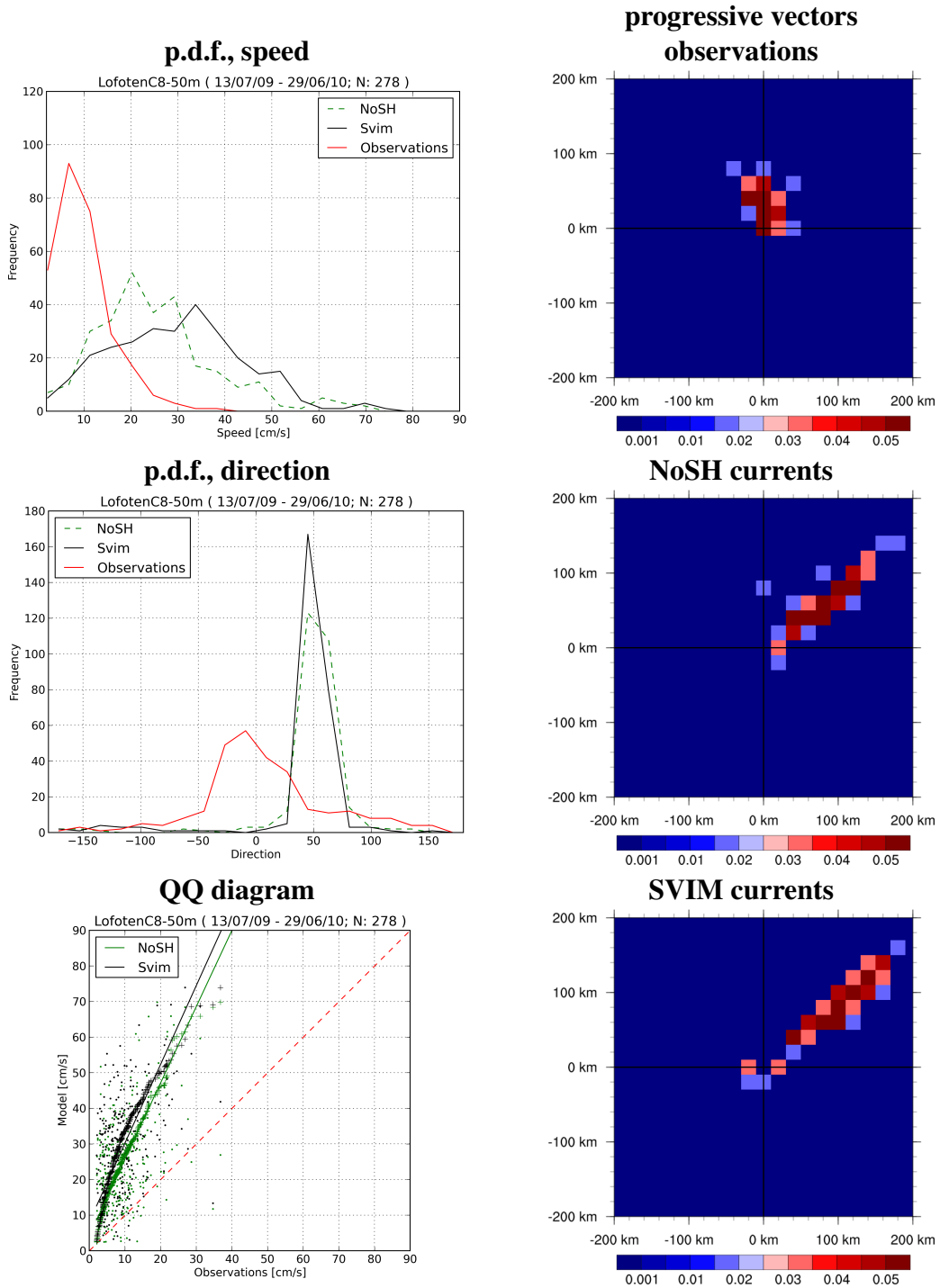
3.2.7 Lofoten C6



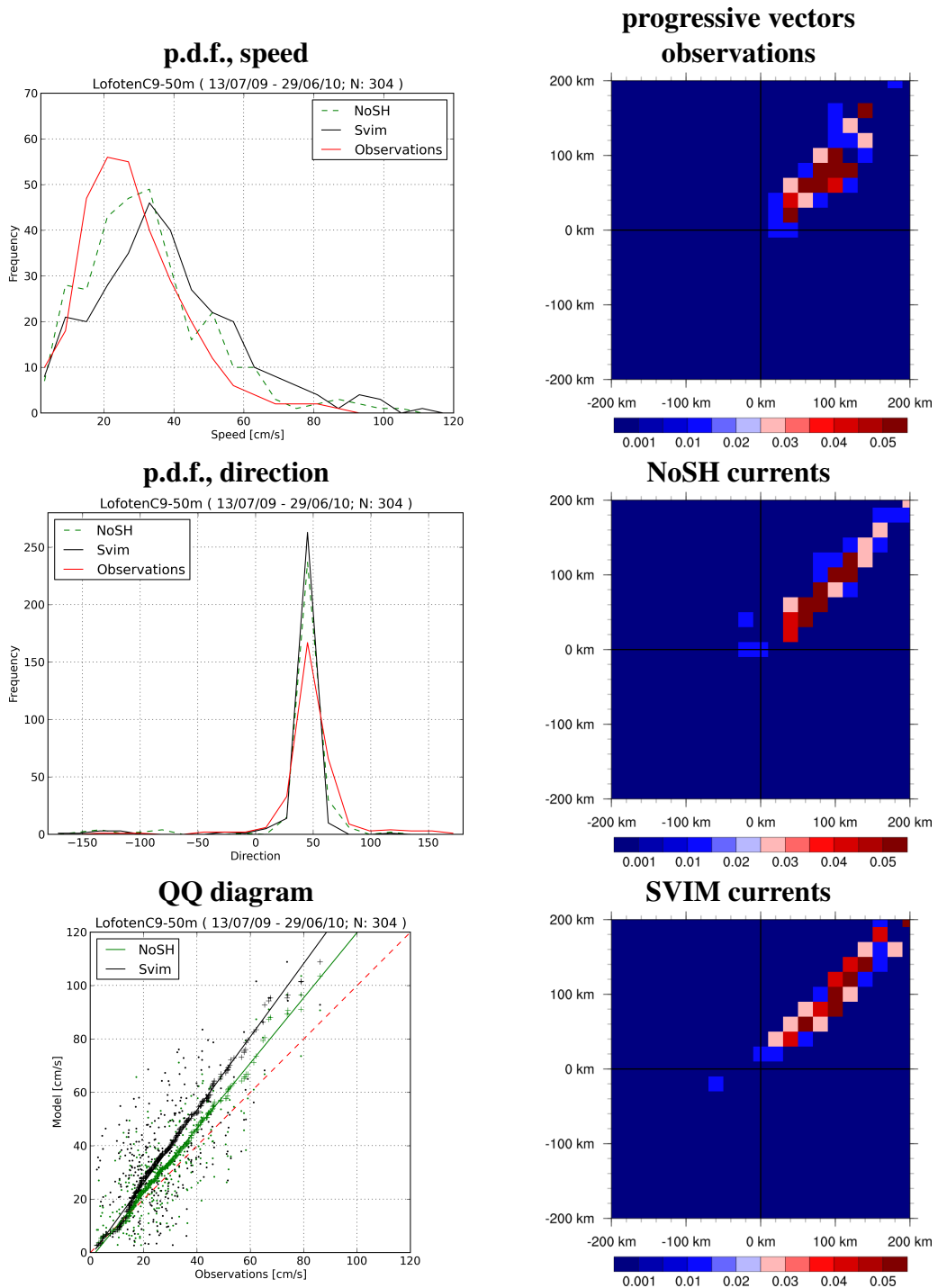
3.2.8 Lofoten C7



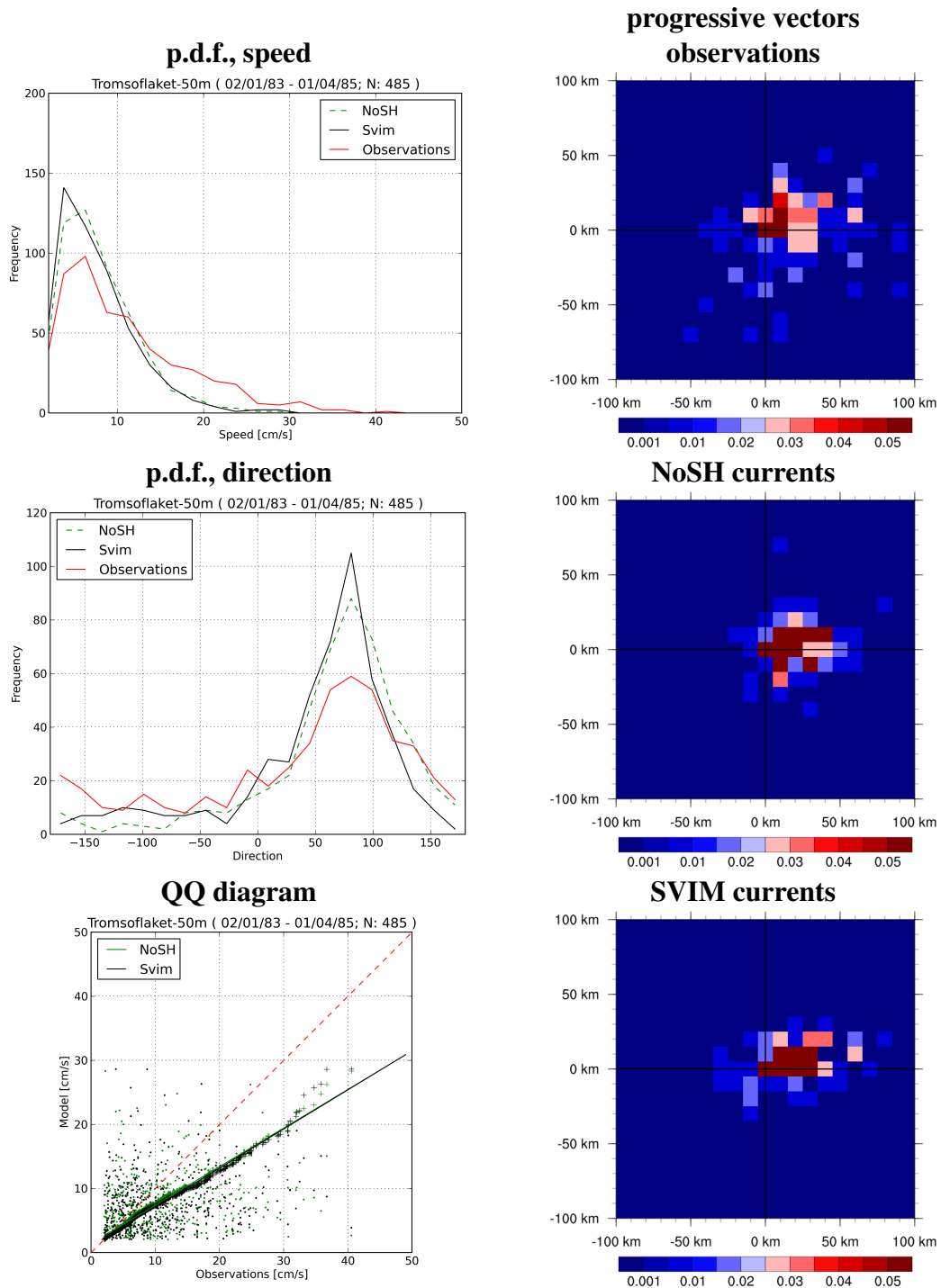
3.2.9 Lofoten C8



3.2.10 Lofoten C9



3.2.11 Tromsoflaket



4 Discussion

First, we note that results for match-ups in time on the qq plots reveal that the present set of simulations display poor predictive skills. Given the small scales of a few km that dominate instantaneous distribution of circulation features, and the complete absence of corresponding observations, this is not surprising.

When investigating the statistics from the qq plots, as given by the results in Tables 1 and 3, we find that the slopes from the NoSH simulation results are closer to 1 for nearly all stations than the corresponding slopes from the SVIM results. We also note that the mean deviation of the qq curve from the linear least square representation is generally smaller for the NoSH results than for SVIM results. Nevertheless, the differences between the representation of the observation statistics from the two simulations is mostly small. The largest differences are in the results for IMR station CM5, and in the deviation at Lofoten C8. In both of these cases, the NoSH results are an improvement over those from SVIM.

Next, we consider the summary of results from the computation of progressive vectors, as given by Tables 2 and 4. With the exception of CM5, results for the IMR stations from SVIM are slight improvements over NoSH results. However, for many of the Lofoten stations (C1,2,6-9), NoSH results constitute notable improvements over the results from SVIM.

The rightmost columns which give non-dimensional offsets from the mean observed progressive vector end points. We note that by this measure, results for the IMR stations are good, while particular problems is seen for the Lofoten stations near the shelf break. These stations, particularly Lofoten C6 and C8, have much too high velocities in the simulations, and more so in SVIM than in NoSH. The same conclusion can be drawn from the qq plot statistics, where regression line slopes are ~ 1 for the IMR stations, while slopes for Lofoten C6 and C8 are ~ 2 .

The record from the IMR stations are much longer than those from the offshore industry stations. Hence, the statistics from the IMR sections are likely better quantifications of the representativeness of the model results. So it is encouraging that the most accurate model statistics are attained for the IMR stations. We note in particular that the qualitative changes from one of these stations to another is well reproduced by the distribution of end positions of the progressive vectors, and the change in scatter of end point distributions.

Nevertheless, it is very unlikely than the improved quality of the IMR positions is pri-

marily due to representativeness. It is much more likely that the model quality depends significantly on its ability to reproduce the local circulation statistics which is very different from one region to another. Above, the contrasts between the result from the IMR stations along the Barents Sea opening with those near the shelf break off Lofoten were discussed. We also remark that model results for the Lofoten stations C3 and C5, furthest inshore of the shelf break are more similar to the observations than those near the shelf break.

Finally, the model results for the stations Norne and GjØa to the south of the Lofoten archipelago reveal that both simulations have skill in reproducing the observed circulation statistics. Note *e.g.* that the non-dimensional mean end point offsets are of similar magnitude as those from the IMR stations. The SVIM results are marginal improvements over those from NoSH. For TromsØflaket to the north of Lofoten the results are similar, but here, NoSH is marginally better than SVIM.

This leads us to conclude that the intensity of the Norwegian Atlantic Current in the vicinity of the shelf break is much too strong in both simulations. Elsewhere, the ocean circulation statistics given by the model results are fair to good representations of the observed statistical distributions.

Acknowledgements

This work has been performed as part of the project *Sustainable management of renewable resources in a changing environment: an integrated approach across ecosystems (SUSTAIN)* which is funded by the Research Council of Norway. Ocean current observations were made available by the Institute of Marine Research, and Statoil ASA (offshore industry stations). The SVIM project was funded by the Research Council of Norway under contract 196685/S40, with computer resources allocated by NOTUR under contract nn9146k. The NoSH project was funded by Statoil ASA under contract 45002815652. The maps, and figures displaying distribution of end positions of progressive vectors, were made using the NCAR Command Language (NCAR , 2014).

References

Lien, V.S., Y. Gusdal, J. Albreten, A. Melsom, F. Vikebø (2013): Evaluation of a Nordic Seas 4 km numerical ocean model hindcast archive (SVIM), 1960-2011. *Fisken og havet*, **7**, 82 pp.

The NCAR Command Language (Version 6.1.0) [Software]. (2014). Boulder, Colorado: UCAR/ NCAR/CISL/VETS. doi:10.5065/D6WD3XH5

Røed, L.P., Lien, V., Melsom, A., Kristensen, N.M., Gusdal, Y., Ådlandsvik, B., Albreten, J. (2015): Evaluation of long-term hindcasted Norwegian Sea currents and hydrography. *MET report 13/2015*, Norwegian Meteorological Institute. NN pp.